

IR Laser Absorption and Modeling Studies of Hydrocarbon Flames  
Inhibited by Candidate Halon Replacement Compounds

Robert G. Daniel<sup>a</sup>, Kevin L. McNesby, and Andrzej W. Miziolek

U.S. Army Research Laboratory  
AMSRL-WT-PC  
Aberdeen Proving Ground, MD 21005-5066

Donald R.F. Burgess, Jr., Phillip R. Westmoreland, Wing Tsang,  
and Michael R. Zachariah

Chemical Science and Technology Laboratory  
National Institute of Standards and Technology  
Gaithersburg, MD 20899

Abstract

The search for viable replacement fire extinguishing compounds for the presently used Halons 1301 and 1211 has been fully underway for some time. A successful replacement compound has to satisfy a number of criteria, including superior fire extinguishment characteristics. Recent advances in combustion science have opened up the possibility of identifying the detailed physical and chemical properties that are responsible for fire inhibition and extinction.

We report in this paper some early results of a coordinated experimental and detailed kinetic computer modeling research effort aimed at identifying the fundamental aspects of flame inhibition. The experiments involve the use of infrared Tunable Diode Laser (TDL) absorption spectroscopy to measure temperature, major, and minor species profiles in a low pressure laminar premixed flame. The detailed kinetic model incorporates a comprehensive fluorine flame chemistry mechanism that was developed recently at NIST. The experiments and modeling involve a number of inhibiting compounds including  $CF_3H$ ,  $CF_2H_2$ , and  $C_2F_6$  that were doped up to 1% in  $CH_4/air$  and  $CH_4/O_2$  stoichiometric flames.

This work indicates that each inhibiting compound exhibits a unique behavior in both experimental and computational results with respect to flame structure and adiabatic flame speed characteristics. In addition, the flame models are accurately predicting the chemical pathways of agent decomposition in which the  $CF_2$  radicals are implicated in the formation of long-lived toxic intermediate species such as  $CF_2O$ . Overall, our results indicate that the detailed chemical kinetic models have the potential for not only predicting the relative fire extinguishment properties of new Halon replacement compounds, or their mixtures, but also to predict the possible formation of toxic compounds during their use in actual fires.

Introduction

The banning of ozone depleting compounds such as the **CFCs** and Halons by the Montreal Protocol and its subsequent amendments has created a significant challenge to the user communities heavily dependent on these compounds. The DoD

is significantly dependent on Halons 1301 ( $\text{CF}_3\text{Br}$ ) and 1211 ( $\text{CF}_2\text{ClBr}$ ) as fire extinguishing agents particularly due to their high performance against very vigorous military-type fires. The urgency of the situation has increased now that the production and sale of Halons has been banned as of 1 January 1994. Most researchers in the Halon replacement compound field would agree that the search for successful replacement agents has been surprisingly difficult with no clear winners yet in sight.

Part of the difficulty of the present situation can be explained by the fact that serious research on the fundamental nature of flame inhibition stopped in the **mid-1980s**, presumably after Halon 1301 was found to be an acceptable agent for a variety of civilian and military applications. Up to that point, there had been a considerable amount of fundamental research that was carried out in various laboratories.<sup>1</sup> The modeling aspect of flame inhibition was culminated by a seminal paper by Westbrook that modeled  $\text{CF}_3\text{Br}$  inhibition and compared modeling results with available experimental data using an extensive bromine and fluorine chemistry **base**.<sup>2</sup> In this work Westbrook proposed that bromine from 1301 suppresses flames by removing H atoms via a catalytic mechanism, whereas the fluorine atoms also remove H-atoms, but not as efficiently. Clearly, a fundamental understanding of flame inhibition should be a major benefit to the Halon replacement problem. In fact, recent advances in combustion science in both experimental flame diagnostics and in detailed kinetic modeling offer the promise of expanding on the earlier work and significantly increasing this sought-after basic understanding. This paper presents results of preliminary experimental and modeling research aimed at developing further insight into the nature of flame inhibition. Our work is part of an extensive effort in the United States by many laboratories on flame inhibition **research**.<sup>3-10</sup> Due to the world-wide significance of the Halon problem, there is also a substantial research effort underway in Europe called SUBSTHAL which is under the sponsorship of the European Community Environmental Programme.<sup>11</sup>

## Experimental

### A. Apparatus

The experimental apparatus may be **divided** into three sections (see Figure 1). These are the low pressure burner **assembly**, the gas handling system, and the optical probe system. The low pressure burner assembly consists of a stainless-steel low pressure flat flame burner (McKenna Industries, Inc.) mounted inside an evacuable chamber (Fig. 2). The low pressure flat flame burner houses a 6 cm diameter circular sintered stainless steel frit through which combustion gases flow and upon which the flame is supported. Premixed combustion gases flow into the underside of the burner and enter a final mixing section immediately below the burner frit. Surrounding the burner frit is a 2 cm wide fritted annulus through which a shroud gas may be flowed.

The burner is mounted on a translating stage which in turn is mounted on a rotatable linear motion feedthrough device, providing a complete range of motion within the burner chamber. The burner chamber is a cylindrical stainless steel chamber **36** inches high by 13 inches in diameter. The chamber has four optical ports, equipped with 1 mm diameter LiF windows, separated by 90 degrees, which lie in a plane 10 inches above the base of the chamber. The 1 mm diameter windows define the minimum spatial resolution and linearity of the line-of-sight

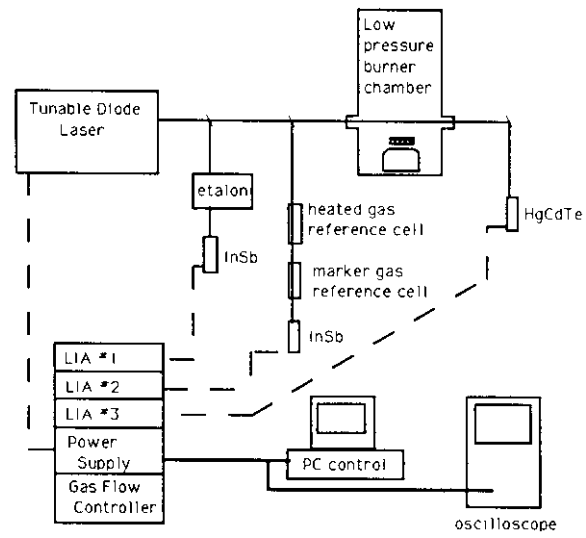


Figure 1 Schematic diagram of the experimental apparatus

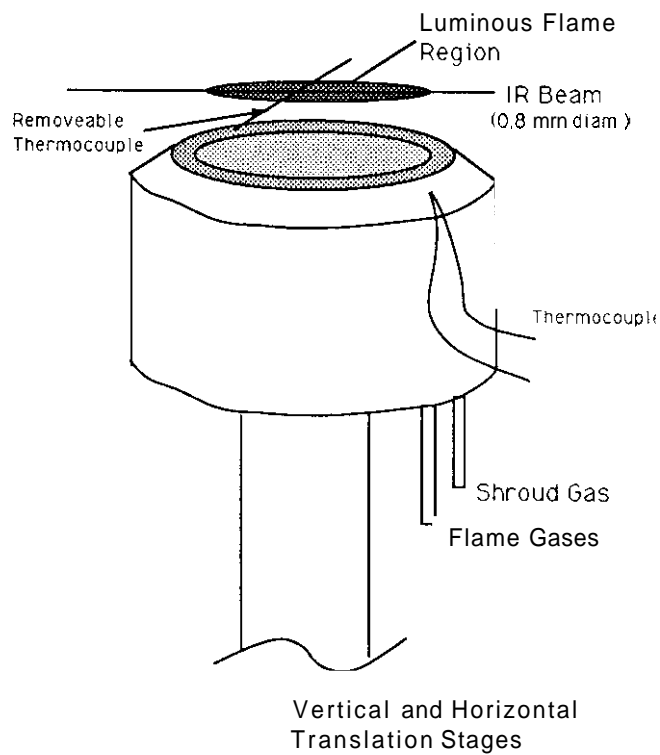


Figure 2. Close up view of the burner head assembly

probe beam which passes through the chamber. The burner chamber is also equipped with a 4 inch diameter hinged-door viewport which is used to visually monitor the flame and through which the flame is lit.

The gas handling system consists of a flow metering system used to regulate fuel, oxidizer and shroud gas flow into the low pressure burner and an exhaust/pressure monitoring system used to control ultimate pressure within the chamber. The fuel, oxidizer and shroud gas flows are controlled by an MKS model 147B flow controller. Inhibitant compounds are added to the premixed fuel and oxidizer via a rotameter which has been calibrated with a Wet Test Meter. Pressure within the chamber is monitored by an MKS type 390 capacitance manometer which samples the pressure at the base of the low pressure chamber. Combustion gases are mixed at a "tee" just prior to entering the low pressure burner chamber.

Exhaust gases are removed from the top of the burner chamber by a Leybold model SV-100 high capacity vacuum pump. Downstream from the chamber and in-line with the pump is an MKS type 253A butterfly valve used for coarse pressure control. Fine pressure control is regulated by an air bleed valve located between the pump and the butterfly valve. This arrangement is capable of maintaining the pressure in the chamber to within several millitorr of a desired pressure over the several hours necessary to obtain a concentration profile for a given species.

Optical probing of the flame is accomplished using a Tunable Diode Laser (TDL) spectrometer system manufactured by Laser Photonics, Inc. The TDL system consists of the laser assembly, monochromator/mode selection system, beam-steering optics, and detector and data collection systems. The laser assembly consists of a single crystal lead-salt diode laser mounted on a liquid-nitrogen cooled flange. Coarse laser tuning is accomplished by back-heating the flange mounted diode laser. Fine tuning of the laser (typically over a  $0.2 \text{ cm}^{-1}$  range for an individual scan) is accomplished by varying the injection current applied to the laser diode.

The multi-mode laser beam is collected by a collimating parabolic steering mirror and directed into a grating monochromator. The monochromator provides coarse ( $\sim 0.5 \text{ cm}^{-1}$ ) frequency and mode selection of the diode laser output, and mechanically chops the beam to enable lock-in detection. Upon exiting the monochromator, the beam enters the beam-steering assembly. In this assembly, the beam passes through two consecutive beam splitters. The reflected portion of light from the first beamsplitter is directed to a passive confocal etalon and then to a liquid nitrogen cooled HgCdTe detector. Etalon fringe spacing is used in the scan mode to determine precise frequency calibration. The reflected portion of light from the second beam splitter is directed through an optical cell containing a reference gas and then to a second liquid nitrogen cooled HgCdTe detector. The reference gas spectrum is used to determine the absolute frequency of the laser light emitted by the diode. The light which has been transmitted by both beamsplitters is then directed to a parabolic mirror which brings the  $\sim 1 \text{ mm}$  collimated laser beam to a focus at the center of the low pressure chamber. Upon exiting the chamber, the light is collected by an ellipsoidal mirror and focused on a third liquid nitrogen cooled HgCdTe detector. The output of the etalon, reference, and low pressure burner detectors is processed using lock-in detection controlled by a personal computer.

Since the diode laser probe beam is always focused at the center of the low pressure chamber at a height defined by the 1 mm windows on the chamber, spatial profiling is accomplished by moving the burner within the chamber relative to the IR beam position. Typically, eight scans are averaged at a given burner position, with each  $0.2 \text{ cm}^{-1}$  range scan taking about 20 seconds. The burner is then translated (horizontally or vertically), and the scan process repeated until the profile has been completed.

Thermocouple measurements of flame temperatures are done using Pt/10%Pt/Rh fine wire (5 micron) thermocouples which have been sheathed with an YtO/BeO ceramic. The high emissivity of the sheath reduces the internal temperature of the thermocouple (necessary because the hottest portion of the flame exceeds the melting point of platinum). Secondly, the sheath minimizes errors caused by platinum catalyzed reactions occurring at the thermocouple surface. The method of coating of the thermocouples and of calculating the emissivity correction for the YtO/BeO sheath has been described previously". The flame temperatures measured by the IR two-line absorption and thermocouple techniques agree to within the experimental error.

All gases were supplied as spectral grade, used as supplied by the manufacturer, without further purification. The fuel, oxidizer, and shroud gases ( $\text{CH}_4$ ,  $\text{O}_2$ ,  $\text{N}_2$ ) were from Matheson, Inc. The  $\text{CF}_3\text{I}$  was from PCR Gases Inc. The fluoromethanes and the  $\text{CF}_3\text{Br}$  were also from Matheson, Inc.

## B. Data Analysis

Line of sight spectra through the low pressure flame were ratioed to a line of sight spectrum through the evacuated chamber to account for the nonlinearity of the diode output. A new background spectrum was recorded prior to each lighting of the flame. Temperature and species concentrations of CO were obtained using two-line thermometry. Errors due to the line of sight technique were estimated using computed tomography, and found to be within the maximum estimated error of the temperature and concentration measurement (less than 10%).

The method of two-line thermometry<sup>13</sup> calculates the temperature of the flame and species concentration from a ratio of the intensities of two infra-red transitions originating from different vibrational levels. Two hot band transitions ( $\nu'' > 0$ ) are used to eliminate saturation effects and minimize interference from cold gas outside the flame region. The ratio of the integrated absorbance is proportional to and compared to a calculated ratio of the transition line strengths. The calculations account for the temperature dependence of the individual linewidths and of the line strengths of the individual transitions.

The ratio of the transition intensities is obtained from a fit of the experimental transmittance spectra by a non-linear least squares fitting routine<sup>14</sup> to a model which uses the calculated line strengths and a Voigt profile for the lineshape. The goodness of fit is measured by the Chi Squared test. The ratio obtained from the fit is used to calculate the temperature of the flame and the concentration of the absorbing species, presently CO. The temperatures obtained have an error of  $\pm 40$  K. Typical temperature profiles are shown in Figure 3. In this figure it is seen that the temperature profile first increases for 0.5%  $\text{CHF}_3$  (solid circles) and then decreases for 1.0%  $\text{CHF}_3$  (open inverted triangles). This lowering of temperature is attributable to the inhibitive

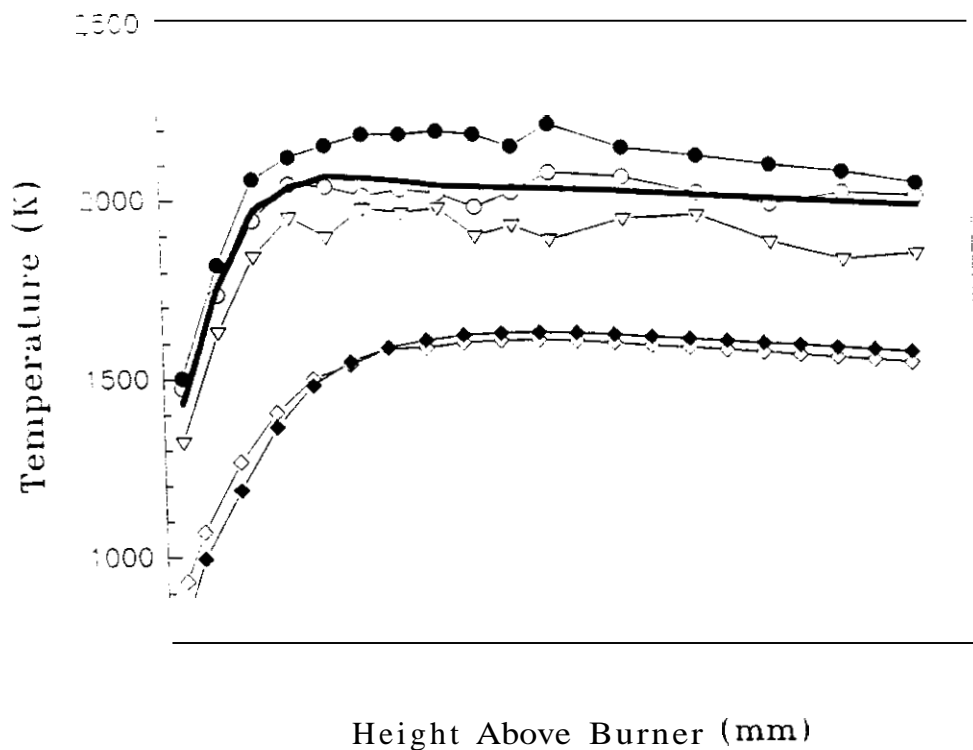


Figure 3. Plot of temperature vs. height above burner for methane/oxygen flames (see text for details).

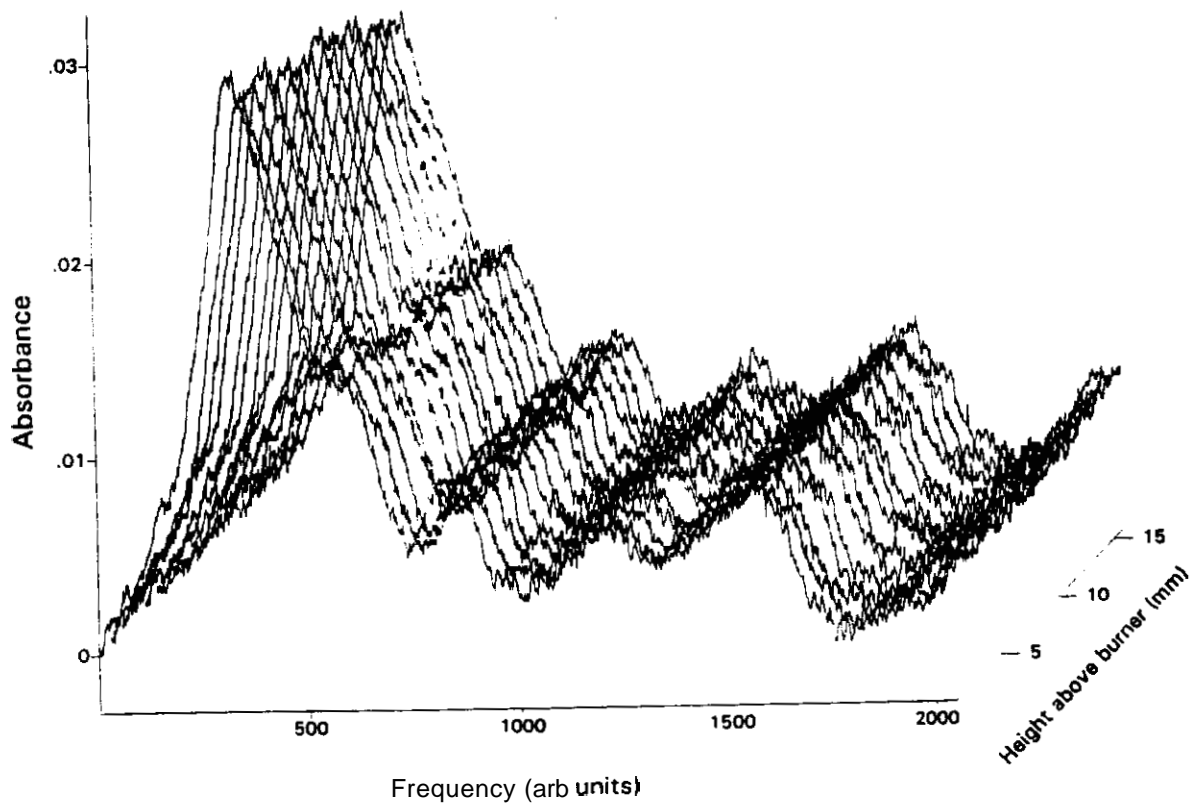


Figure 4. Plot of absorbance of  $\text{CF}_2\text{:O}$  vs. height above burner for a 20 torr flame inhibited with  $\text{CF}_3\text{H}$ .

action of CHF, affecting the chemical kinetics of the combustion process, The open circles are for 0.25% CHF, and the solid line is the uninhibited flame temperature. The bottom two traces are offset by approximately 350 K for clarity and represent thermocouple data for the uninhibited flame (open diamonds) and for 0.4% CF<sub>3</sub>I. Figure 4 shows the measured absorbance of CF<sub>2</sub>O as a function of height for a 20 Torr CH<sub>4</sub>/O<sub>2</sub> stoichiometric flame. As can be seen the spectra indicate that CF<sub>2</sub>O is not being consumed readily in the flame, which is in general agreement with modeling calculations (see discussion below)

### Modeling Results and Discussion

The modeling portion of our work is based on an extensive fluorine kinetic flame mechanism that was developed recently by scientists at NIST.<sup>8</sup> A most important ingredient of this work has been the development by the same group of a state-of-the-art graphical post processor for the Sandia CHEMIN-based kinetic codes including PREMIX. The details of the fluorine flame mechanism will not be presented here (see Ref. 8 for these details), rather, we will concentrate on describing the results of the application of the model for our low pressure flame experiments.

Figure 5 shows the results of model calculations of the adiabatic flame velocity for a number of inhibiting compounds in a 20 Torr stoichiometric CH<sub>4</sub>/air flame. These results are based on running the PREMIX flame code in the freely propagating flame mode. As mentioned above, the fluorine mechanism that was used was the one developed at NIST for a fuel-lean atmospheric pressure flame. The model calculations shown in Figure 5 do not contain the necessary corrections for rate constant values at low pressure. We are in the process of incorporating these corrections into the model. It is clear from the results shown in Figure 5 that each of the four suppression compounds exhibits a unique flame inhibition behavior.

Figures 6 and 7a-c show the modeling-generated reaction paths for all four of the inhibiting compounds at a 1% dopant level in CH<sub>4</sub>/air 20 Torr stoichiometric flames. A careful comparison of the pathways reveals the unique behavior for each inhibiting compound. In particular, we can see that the compounds C<sub>2</sub>F<sub>6</sub>, CHF<sub>3</sub>, and CF<sub>4</sub> all indicate the importance of the CF<sub>2</sub>O formation channel, whereas for the CH<sub>2</sub>F<sub>2</sub> case, this channel is less important. These results are consistent with those found by the NIST group for the fuel-lean atmospheric pressure flame.<sup>8</sup> Another interesting comparison involves the CF<sub>3</sub>I, inhibitor (Figures 7c-d) in CH<sub>4</sub>/air and CH<sub>4</sub>/O<sub>2</sub> simulated flames. What can be readily seen is the importance of temperature both in the destruction mechanism for the parent compound, as well as for the destruction of the toxic CF<sub>2</sub>O molecules (the oxygen flame is much hotter than the air flame). It should be noted here that we set a threshold limit of 5% relative reaction magnitude as our criterion for inclusion of a particular path in the figures.

### Conclusions

It is clear that the TDL absorption technique works well for flame structure studies of inhibited flames. This technique is particularly well-suited for low pressure flame studies where absorption lines sharpen up and spectral overlap due to pressure broadening is minimized. Although not as

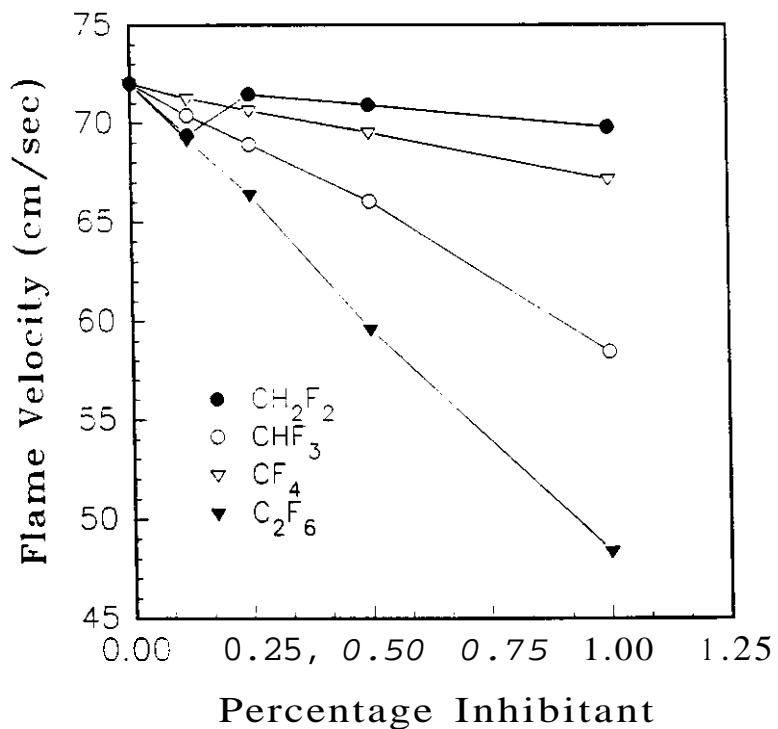


Figure 5. Adiabatic flame velocities vs. concentration of inhibitor for a stoichiometric 20 torr methane/air flame.

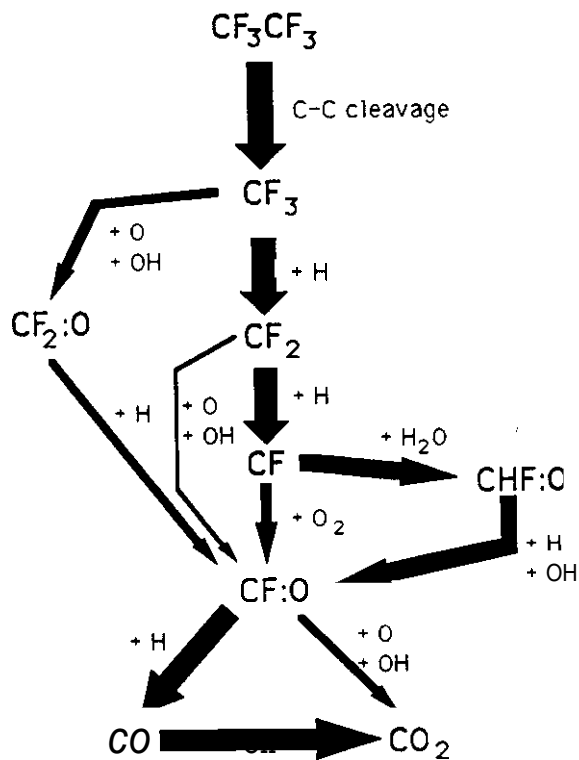


Figure 6 Reaction paths in a 20 torr stoichiometric methane/air flame with 1% C<sub>2</sub>F<sub>6</sub> added



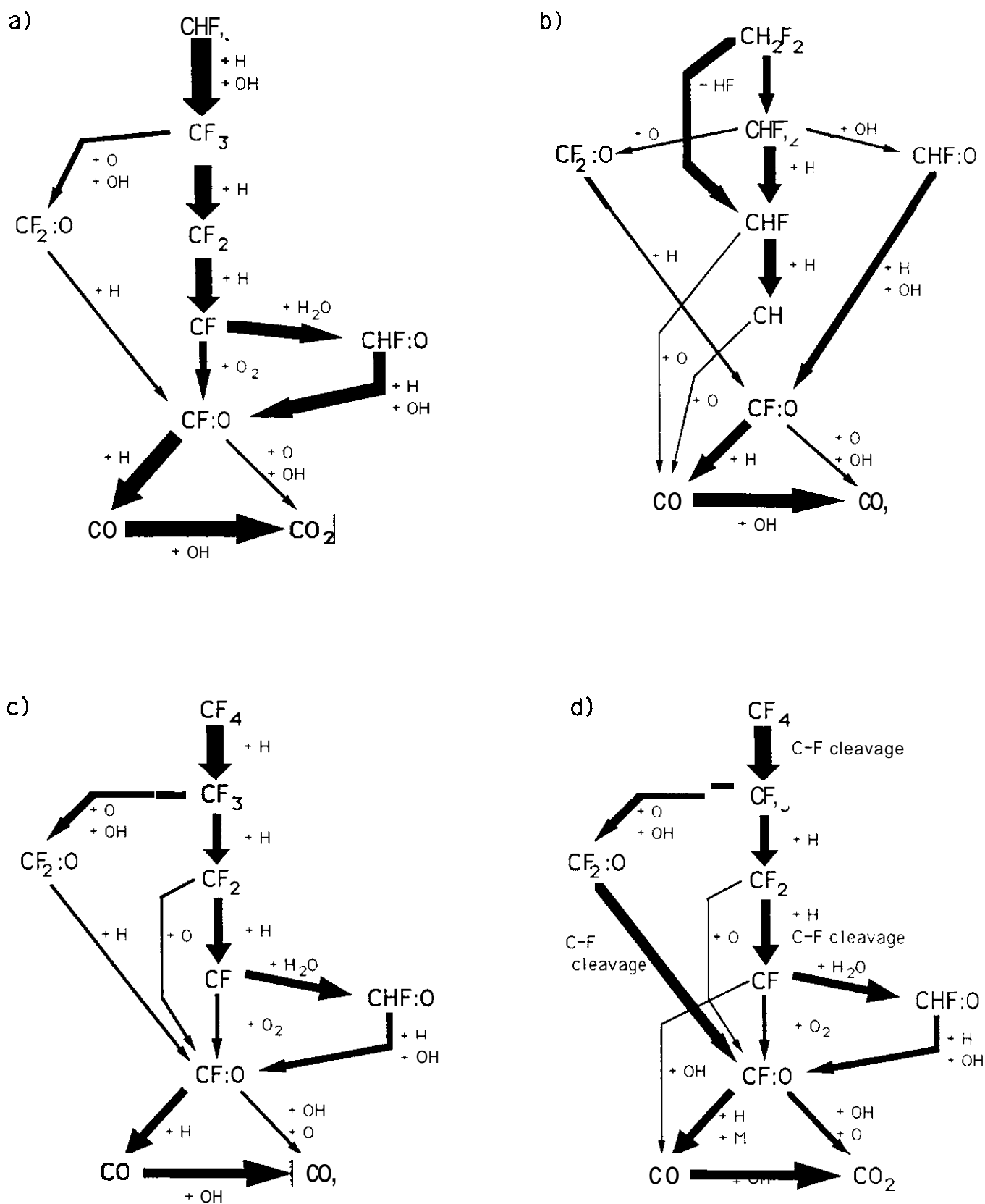


Figure 7 Reaction paths in 20 torr stoichiometric flames a) methane/air with 1% CHF<sub>3</sub>, b) methane/air 1% CH<sub>2</sub>F<sub>2</sub>, c) methane/air with 1% CF<sub>4</sub>, and d) methane/oxygen with 1% CF<sub>4</sub>

sensitive to all of the important major and minor flame species as compared to mass spectrometry, it can detect a significant number of stable and reactive species, as well as determine the flame temperature. The TDL technique, in fact, has some important advantages over mass spectrometry. These include an unambiguous determination of species identity due to high resolution infrared spectroscopy (mass spectrometry is always concerned with ion fragmentation), and the fact that the TDL technique is truly non-intrusive (mass spectrometric sampling always involves an intrusive probe). As far as we can tell, our present work with the TDL technique represents the most extensive application to date of infrared absorption spectroscopy to flame structure research.

The experimental and modeling results so far indicate that each candidate Halon replacement compound exhibits a unique flame inhibition behavior with respect to effect on the adiabatic flame temperatures and velocities, as well as on the reaction pathways. Fundamental studies such as these represent the only means of developing insight into why each compound behaves in a unique manner with respect to flame inhibition.

Our modeling results show that detailed kinetic flame mechanisms which approach 1000 elementary reactions are quite tractable and that flame modeling runs of this magnitude can be done routinely on workstations. This is important for the next step of modeling development where bromine and iodine chemistry are added to the existing fluorine chemistry. It is important to remember that once these very large and laborious mechanisms are validated through comparison with experimental flame structure measurements, they will subsequently be significantly reduced via sensitivity analyses. Therefore, once this latter stage is reached, these reduced chemistry models will be very useful as engineering aids for workers in the survivability laboratories.

The results of the work presented in this paper point out the importance of a number of flame species in the reaction pathways of the inhibitor compounds. In particular, our results confirm the earlier work at NIST on lean atmospheric pressure flames which indicates that  $CF_3$  and  $CF_2O$  are very important players in the inhibition mechanisms of these methane flames. In addition, our results show the strong temperature effect on the destruction of the toxic compound  $CF_2O$ . It is therefore clear that studies such as ours are shedding important new light on the nature of inhibition behavior of a number of candidate replacement compounds.

#### Acknowledgement

Research support from the Strategic Environmental Research and Development Program (SERDP) is gratefully acknowledged. The development of the fluorine flame mechanism by NIST was supported by the DoD/FAA Agent Screening for Halon 1301 Aviation Replacement Program.

a. NRC Postdoctoral Research Associate

#### References

1. R.N. Gann, Halogenated Fire Suuuressants, ACS Symposium Series, vol. 16, American Chemical Society, Washington, DC, 1975.

2. C.K. Westbrook, Combustion Science and Technology, Vol. 34, p. 201, 1983
3. G.T. Linteris, Proceedings of this meeting and references therein
4. G.W. Gmurczyk et al., Proceedings of this meeting and references therein
5. V.I. Babushok et al., Proceedings of this meeting and references therein
6. A.E. Finnerty, Proceedings of this meeting and references therein
7. J.A. Manion et al., Proceedings of this meeting and references therein
8. D.R.F. Burgess, Jr. et al., Proceedings of this meeting and references therein.
9. A. McIlroy et al., Proceedings of this meeting and references therein
10. A. Hamins et al., Proceedings of this meeting and references therein
11. F. Baronnet, Nancy, France, private communication.
12. J.H. Kent, Combustion and Flame, Vol. 14, p. 279, 1970.
13. S.M. Schoenung and R.K. Hanson, Combustion Science and Technology, Vol.24, p. 227, 1981; X. Ouyang, P.L. Varghese, and D.S. Cline ~~in Advances In Laser Science IV~~, J.L. Gole, D.F. Heller, M. Lapp, and W.C. Stwalley, Eds. (American Institute of Physics, New York, 1989), p. 750.; X. Ouyang and P.L. Varghese, Applied Optics, Vol. 29. p. 4884, 1990.
14. P.R. Bevington, Data Reduction and Error Analysis for the Physical Sciences, McGraw-Hill, New York, 1969.

